Topical application of Heparanase-1 facilitates bone remodeling during the healing of bone defects in a mouse model

Po-Yu Chiu[a], Wei-Chun HuangFu[b], I-Hsuan Liu[c,d,e], Ya-Pei Chang[a,*]

[a]Institute of Veterinary Clinical Science, School of Veterinary Medicine, National Taiwan University, Taipei, Taiwan, ROC; [b]The Ph.D. Program for Cancer Biology and Drug Discovery, College of Medical Science and Technology, Taipei Medical University, Taipei, Taiwan, ROC; [c]Department of Animal Science and Technology, National Taiwan University, Taipei, Taiwan, ROC; [d]Research Center for Developmental Biology and Regenerative Medicine, National Taiwan University, Taipei, Taiwan, ROC; [e]School of Veterinary Medicine, National Taiwan University, Taipei, Taiwan, ROC

Abstract

Background: Although previous studies have suggested a stimulatory role of heparanase in physiological bone turnover, the potential therapeutic role of heparanase in bone healing has not been elucidated. The purpose of this study was to assess the effect of topical application of heparanase-1 on bone healing.

Methods: Two different dosages of recombinant mouse heparanase-1 and vehicle control were prepared and delivered via an osmotic pump to provide continuous topical infusion of the therapeutic reagent in a mouse bone defect model at the distal femoral metaphysis. The bone healing progress was evaluated by micro-computed tomography and histological examination at 7, 14, and 21 days after the bone defect was created.

Results: The peak of trabecular bone generation was achieved earlier than anticipated with the use of heparanase as measured by medullary bone volume fraction and trabecular number observed in micro-computed tomography, while the remodeling of trabecular bone to cortical bone was also achieved earlier than anticipated with the use of heparanase as measured by connectivity density. Histopathological observation revealed a higher frequency of the presence of cartilaginous tissue in the heparanase-treated groups. Both bone mineral density and cortical bone volume fraction showed the best healing outcome with low-dose heparanase, implying a biphasic effect of its mode of action.

Conclusion: These results indicated that with the appropriate dose of topical heparanase-1, the progress of bone healing could be accelerated *in vivo*.

Keywords: Bone regeneration; Heparan sulfate; Heparanase

1. INTRODUCTION

Bone tissue is one of the best regenerative tissues in adults, which is capable of healing with minimal or no scar tissue formation following a defect or fracture. Immediately after the occurrence of injury on bone tissue, blood clot and hematoma derived from the hemorrhage act as a scaffold for callus formation and as reservoirs trapping various inflammatory cells, cytokines, and growth factors, such as bone morphogenic protein (BMP)-2.[1] These cytokines and growth factors in turn recruit more inflammatory cells and mesenchymal stem cells (MSCs), which enhance the accumulation of growth factors and later contribute to osteoinduction for the regeneration of the injured bone tissue via intramembranous ossification or endochondral ossification.[1] Subsequently, osteoblasts are recruited to give rise to woven bones, while chondroclasts transform the fibrous tissue and chondrocytes into callus.[2] A final bone remodeling transforms callus and woven bones into compact lamellar bone at the cortices and restores the marrow cavity in the center.[1]

Heparan sulfate (HS) proteoglycans (HSPGs) are ubiquitous macromolecules associated with the extracellular matrix (ECM) and cell membranes in animals. Covalently attached to the core proteins of HSPGs, HS chains can bind to various proteins including chemokines and growth factors and, in turn, can modulate the distribution and bioactivity of these molecules.[3] Many of these chemokines and growth factors are known to play a role in the regeneration of bone tissue, including fibroblast growth factor-2 (FGF2), BMP-2, and vascular endothelial growth factor (VEGF).[4–6] Accordingly, attempts to apply HS to facilitate bone repair have been made but with controversial results.[7–9]

Heparanase (HPSE) is an endo-β-D-glucuronidase that can hydrolyze HS chains at specific sites, and hence, its action results in the degradation and remodeling of the ECM and basement membrane.[10,11] This enzymatic activity can also release the HS-bound growth factors including FGF2 and VEGF and

*Address correspondence. Dr. Ya-Pei Chang, Institute of Veterinary Clinical Science, School of Veterinary Medicine, National Taiwan University, 1, Section 4, Roosevelt Road, Taipei 106, Taiwan, ROC. E-mail address: yapeichang@ntu.edu.tw (Y.-P. Chang).

Conflicts of Interest: The authors declare that they have no conflicts of interest related to the subject matter or materials discussed in this article.

Journal of Chinese Medical Association. (2020) 83: 272-279.

Received September 6, 2019; accepted December 11, 2019.

doi: 10.1097/JCMA.0000000000000261.

potentiate the distribution of these factors.[12,13] Transgenic mice that ubiquitously overexpress HPSE showed markedly increased trabecular bone mass, cortical thickness, and bone formation rate, suggesting that HPSE may be favorable in the regeneration of injured bone tissue.[14] Marrow MSCs are the stem cells responsible for the homeostasis and regeneration of bone tissue,[15] and the expression of HPSE1 in these cells plays a role in the proliferation and migration of marrow MSCs.[16] It is therefore of immense interest to assess the effect of exogenous application of HPSE1 on bone healing.

In the present study, we examined the effect of topical application of HPSE1 on bone healing in a mouse bone defect model by the continuous infusion of recombinant HPSE1. Compared with the conventional fracture model in mice, this model provides an easy, inexpensive, and reproducible method to access the bone healing without additional fixation.[17] In addition to the conventional histopathological assay, we also acquired micro-computed tomographic (μCT) images for three-dimensional (3D) reconstruction to evaluate bone density and other morphometric changes during the regeneration of the bone defects.

2. METHODS

2.1. Animals

C57BL/6 male mice (BioLasco, Taipei, Taiwan) aged 6 weeks were housed in a light-controlled (14-hour light/10-hour dark cycle) and temperature-controlled (25 ± 2°C) environment for 2 weeks before the experiments and provided with food and water *ad libitum*. All procedures in this study were reviewed and approved by the Institutional Animal Care and Use Committee (NTU-102-EL-7).

2.2. Preparation of the recombinant HPSE1

Mouse *HPSE1* cDNA with Myc-FLAG tag at the C-terminal end (OriGene, Rockville, MD, USA) was transfected to HEK293 cells using *Trans*IT-LT1 Transfection Reagent (Mirus Bio, Madison, WI, USA) according to the manufacturer's instructions. The stably transfected cells were selected and maintained in Dulbecco's modified eagle's medium (Invitrogen, Carlsbad, CA, USA) with 10% fetal bovine serum (Biochrom AG, Berlin, Germany), 100 U/mL penicillin, 100 μg/mL streptomycin (Invitrogen), and 800 μg/mL G418 (A.G. Scientific, San Diego, CA, USA). The culture medium was collected every 48 to 72 hours and then concentrated from >45 to 1 mL in Amicon Ultra-15 Centrifugal Filter Units (30 kDa molecular weight cut-off; Millipore, Billerica, MA, USA). The recombinant mouse HPSE1 was then affinity purified by adding 200 μL ANTI-FLAG M2 Magnetic Beads (Sigma-Aldrich, Buchs, Switzerland) according to the manufacturer's instructions. The final elution was carried out using 800 μL of 0.1 M Glycine (adjusted to pH 3 with HCl; Merck, Darmstadt, Germany) and the buffer was swapped with Amicon Ultra-15 Centrifugal Filter Units into phosphate buffered saline (PBS; Invitrogen) for the *in vivo* study or into 1 mL 0.1 M sodium acetate (NaOAc, pH 4.0; Sigma-Aldrich) for enzymatic characterization. The concentration of purified HPSE1 was determined by BCA Protein Assay (Thermo Fisher Scientific, Rockford, IL, USA) according to the manufacturer's instructions.

The enzymatic activity of purified HPSE1 was characterized by the dot blot assay.[16] Briefly, the cell lysate of mouse marrow MSCs, prepared as described previously,[16] was mixed with HPSE reaction buffer (25 mM 4-morpholineethanesulfonic acid, 25 mM $MnCl_2$, 25 mM $MgCl_2$, 1.25 mM $CaCl_2$, 0.5% Triton X, 0.75 mg/mL BSA, pH 7.1) in 1:1 volume ratio as sample mix. The sample mix was then mixed with 0.166, 2.04, 4.166, and 8 ng/μL of HPSE1 in 1:1 volume ratio as reaction mix and then incubated at 37°C for 30 minutes. After incubation, 2 μL of reaction mix was transferred by spotting onto a polyvinylidene difluoride membrane (Hybond-p; GE Healthcare Life Sciences, Marlborough, MA, USA), and the residual intact and fragmented HS glycosaminoglycans were evaluated according to the immunoreactivity against monoclonal antibody 10E4 (1:500; United States Biological, Salem, MA, USA) and 3G10 (1:500; United States Biological) (**Figure 1**).

The drug delivery system used in this study was an implantable osmotic pump (ALZET, Cupertino, CA, USA), which continuously delivered reagents topically through the catheter. To evaluate the effect of different dosages of HPSE1, 0.083 and 2.08 ng/μL HPSE solutions were prepared for doses of 0.5 μg/mouse/d (HPSE1 low-dose group, Low) and 12.5 μg/mouse/d (HPSE1 high-dose group, High). The vehicle control group (Control) contained vehicle (1% dimethyl sulfoxide in normal saline) only without HPSE1.

2.3. Bone defect model and the implantation of osmotic pump

The bone defect model was created as previously described.[17] Briefly, general anesthesia was induced with 4% to 5% isoflurane and maintained with 1.75% to 2% of isoflurane. After appropriate preparation for the operation, a skin incision was made on the lateral side of the distal thigh. The muscles were incised to expose the lateral aspect of the distal femur. A 1.5-mm-deep, 1-mm-diameter cylindrical bone defect was created by a 1-mm drill bit through a single layer of cortical bone and cancellous bone of the metaphysis of the distal lateral femur. To implant the osmotic pump for drug delivery, another small skin incision was made on the lateral hip region. The subcutaneous space on the back was bluntly dissected from the hip incision, and the osmotic pump was implanted. A 25-gauge needle was used to guide the osmotic pump catheter to pass through the submuscular tunnel from the hip region to the bone defect region. After securing the

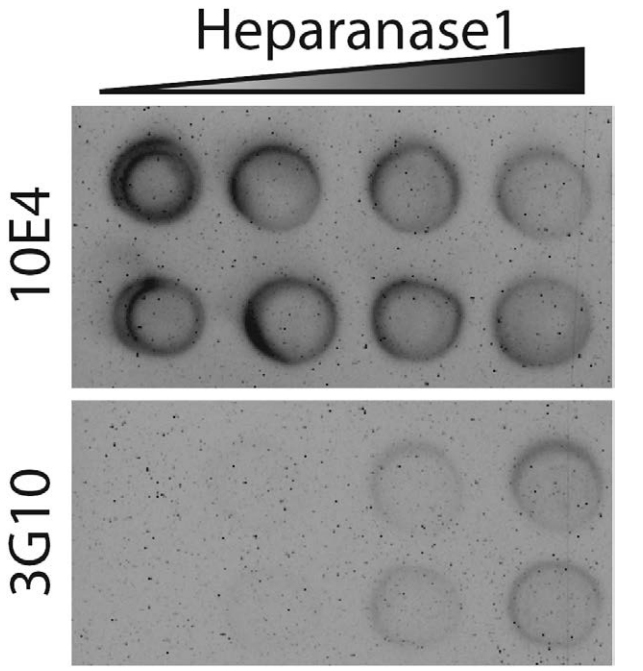

Fig. 1 Recombinant mouse heparanase-1 prepared from stably transfected HEK293 cells is enzymatically active. The dot blot assay showed that recombinant heparanase-1 decreased the immunoreactivity of bone marrow-derived mesenchymal stem cell lysate against 10E4 antibody (intact HS), while increasing the immunoreactivity against 3G10 antibody (fragmented HS) in a dose-dependent manner. HS = heparan sulfate.

pump and catheter, the catheter was cut to allow the opening at the level of the defect. A small quantity of cefazolin (250 mg/mL) was spread onto the subcutaneous region of the surgical wound after closing the muscles. The skin was closed with surgical staples. Gentamicin (1 mg/mL, 0.1 mL/mouse/d, subcutaneous) was administered for 3 days after the surgical procedures. Mice were sacrificed at 1, 2, and 3 weeks post-injury (wpi) (n = 6/group/time point). The right femurs were collected and fixed in 10% formaldehyde for 72 to 96 hours. Before conducting the experiments, all surgical techniques, including surgical approach, the bone defect model, implantation of the osmotic pump, and tissue harvesting, were practiced to standardize conditions. During the experiments, surgical procedures for mice at the same time point were conducted over 2 to 3 continuous days, to further reduce the difference among groups with respect to surgical performance.

2.4. Micro-computed tomography

The collected femurs were scanned at 50 kV/140 μA/3300 ms using the SkyScan 1076 Micro-CT System (Bruker, Billerica, MA, USA) at a pixel size of 9 μm and an acquisition of 225 projections per 180°. The volume of the trabecular bone (BV), tissue volume (TV), trabecular thickness (Tb. Th), trabecular separation (Tb. Sp), trabecular number (Tb. N), connectivity density (Conn.D), and bone mineral density (BMD) were determined by running the CTAn software (Bruker) for evaluation at the region of the defect. The BV/TV ratio indicates the bone volume fraction in the medullary cavity. Tb. Th shows the mean diameter of trabecular bones. Tb. Sp indicates the mean distance between trabecular bones. Tb. N is defined as the number of trabecular bones per unit length. Conn.D measures the degree of connectivity of trabeculae normalized by TV, demonstrating the redundancy of trabecular connections. BMD is calculated from the average attenuation value of the region.[18]

2.5. Histology and histomorphometry

The collected femurs were rinsed with PBS (pH 7), decalcified in 10% EDTA for 3 days, dehydrated, and then embedded in paraffin. Longitudinal 5-μm-thick sections were acquired every 120 μm through lateral–medial orientation and stained with hematoxylin and eosin. The sections were examined and documented under a light microscope (DM2500, Leica Microsystems, Wetzlar, Germany). The section including the center region of the defect was chosen for histomorphometric analysis to evaluate the cortical bone volume fraction by using ImageJ.[19]

2.6. Statistics

All data are expressed as the mean ± SEM. The differences between groups were analyzed with two-way analysis of variance (ANOVA) followed by Bonferroni post-tests. A p value <0.05 was considered statistically significant.

3. RESULTS

Purified recombinant HPSE1 could degrade HS in a dose-dependent manner as shown by the dot blot assay. The reactivity of cell lysates of mouse marrow MSCs against 10E4 (intact HS as the epitope) decreased with the increased level of HPSE1, while the reactivity of cell lysates of marrow MSCs against 3G10 (fragmented HS as the epitope) increased with the increased level of HPSE1 (**Fig. 1**). All operated mice survived through the experimental period without any signs of infection, and the operated legs could begin to bear their body weight within 24 hours. Lameness was not observed at 7 days in all subjects, and no apparent difference among groups was observed.

The 3D reconstruction models from the μCT images enabled the observation of the structural changes in injured bone tissue at 1, 2, and 3 wpi (**Fig. 2**). The boundaries of the defects could clearly be observed at 1 wpi, and the complex spiny texture within the injury areas reflected the formation of the trabecular bones, indicating the middle stage of the bone healing process (**Fig. 2**, dotted circles). This spiny texture within the injury regions was more prominent in the vehicle control group at 2 wpi compared with both the HPSE1-treated groups (**Fig. 2**). At 3 wpi, the surface of the injury areas was largely restored and became smooth, indicating the end stage of remodeling and the reestablishment of cortical bone, while the trabecular bone and dented wound area could still be observed in the control group (**Fig. 2**).

Morphometric analysis of μCT showed significantly higher trabecular bone volume fraction (BV/TV) in the medullary cavity in the HPSE1 low-dose group at 1 wpi compared with the control and HPSE1 high-dose groups, while the BV/TV ratio was significantly higher in the control group compared with both the HPSE1-treated groups after 2 wpi (**Fig. 3A**). A similar trend of dynamic changes could be observed in the Tb. N (**Fig. 3B**).

In the morphological evaluation of the trabecular bones, the dynamic change in Tb. Th as the bone healing progressed was similar to that in the Tb. N (**Fig. 3C**). The Tb. Sp showed an inverse trend where the HPSE1 low-dose group showed significantly higher value at 3 wpi compared with the other groups (**Fig. 3D**). The Conn.D in the control group clearly showed that the complexity of the trabecular bones gradually increased at the early stage and then reduced later as the healing progressed during the remodeling stage (**Fig. 3E**). Interestingly, the Conn.D of the HPSE1 low-dose group was significantly higher than that of the HPSE1 high-dose group at 1 wpi, while this value was significantly higher in the control group compared with both the HPSE1-treated groups at 2 wpi (**Fig. 3E**), suggesting that the dynamic change seemed accelerated in both the HPSE1-treated groups. Notably, the BMD was significantly lower in the HPSE1 high-dose group than in the low-dose HPSE1-treated group (**Fig. 3F**).

A typical histological appearance could be observed in the control group where the fibrous, disorganized, and less stained woven bones (**Fig. 4A**; concave arrow) filled in the medullary cavity with a few calcified trabecular bones (**Fig. 4A**; concave arrowhead) at 1 wpi (**Fig. 4A**). As bone healing progressed, the trabecular bone appeared more abundantly in the medullary cavity and also partially in the cortical defect area with occasional cartilage tissues at the periosteal area, indicating the occurrence of endochondral ossification (**Fig. 4B**) (Table). Later in the healing process, the newly generated cortical bone bridged the defect area at 3 wpi, while the trabecular bones in the medullary cavity were markedly reduced (**Fig. 4C**) (Table).

When compared with the control group at 1 wpi, fibrous tissue was more abundant in the HPSE1 low-dose groups and trabecular bone was considerably more abundant in the HPSE1-treated groups, especially in the high-dose group (**Fig. 4D, G**). At 2 wpi, the trabecular bones filled the cortical defect in both the HPSE1-treated groups, indicating a cortical bridging in the injury region (**Fig. 4E, H**) (Table). In some cases, cartilage tissues (**Fig. 4H**; arrowhead) were also observed adjacent to the defect (Table). At 3 wpi, the morphology of the cortical bridging was more complete in both the HPSE1-treated groups compared with the control (**Fig. 4F, I**). Although cartilage tissues were observed in all groups at 2 and 3 wpi, the occurrence was higher in both the HPSE1-treated groups compared with the control group (Table).

We further morphometrically analyzed the cortical bone volume fraction as an estimation of the cortical bone regeneration. Compared with the control group, the cortical bone volume

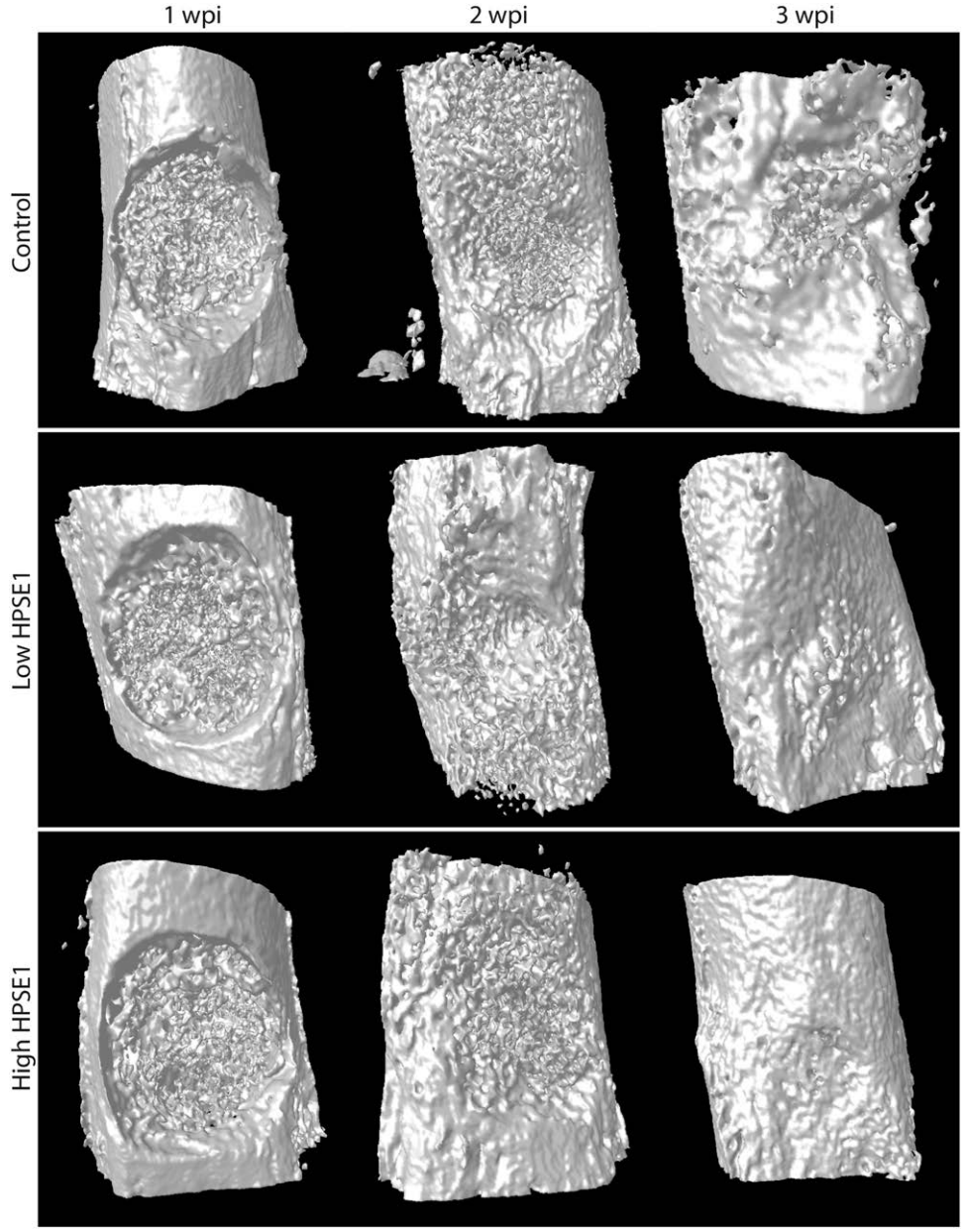

Fig. 2 Three-dimensional reconstruction of μCT images of different treatment groups at 1, 2, and 3 wpi. A cylindrical bone defect could easily be identified at 1 wpi in all three groups with trabecular bones within the region of injury as shown by the grainy texture in the images. As the healing progressed, the boundary of the defect (dotted circles) was not as clear at 2 wpi. Note the smooth surface in both the heparanase-treated groups, suggesting the completion of the cortical bone remodeling, while the injury region in the control group was markedly more dented at 3 wpi. μCT = micro-computed tomographic; HPSE = heparanase; wpi = weeks post-injury.

fraction was significantly higher at both 2 and 3 wpi in the HPSE1 low-dose group and at 3 wpi in the HPSE1 high-dose group (**Fig. 5**). With respect to time-dependent changes, the cortical bone volume fraction increased significantly between 2 and 3 wpi in both the HPSE1-treated groups but not in the control group (**Fig. 5**). There was no significant difference detected between the two HPSE1-treated groups (**Fig. 5**).

4. DISCUSSION

In the present study, we aimed to assess the therapeutic potential of HPSE in bone healing. The therapeutic principles to enhance bone healing include increasing osteogenic cell populations, augmenting osteoinductive stimulus, elevating osteoconductive matrix scaffolds, improving mechanical stability, and enriching vascularization.[20,21] HPSE is a multifunctional molecule that cleaves the HS chain at specific sites and, in turn, may remodel the ECM and adjust the release of HS-binding growth factors such as FGF2, BMP-2, and VEGF to modulate the inflammatory reaction, angiogenesis and osteoblast proliferation, migration, and differentiation.[3,22–24] Therefore, this enzyme may play multiple roles in enhancing bone healing.

Various parameters such as the generation and the complexity of the trabecular bone elevate in the early stage of bone healing while decline as remodeling process in the late stage.[17] In our study, results in **Fig. 3** reflected the progress of bone healing was

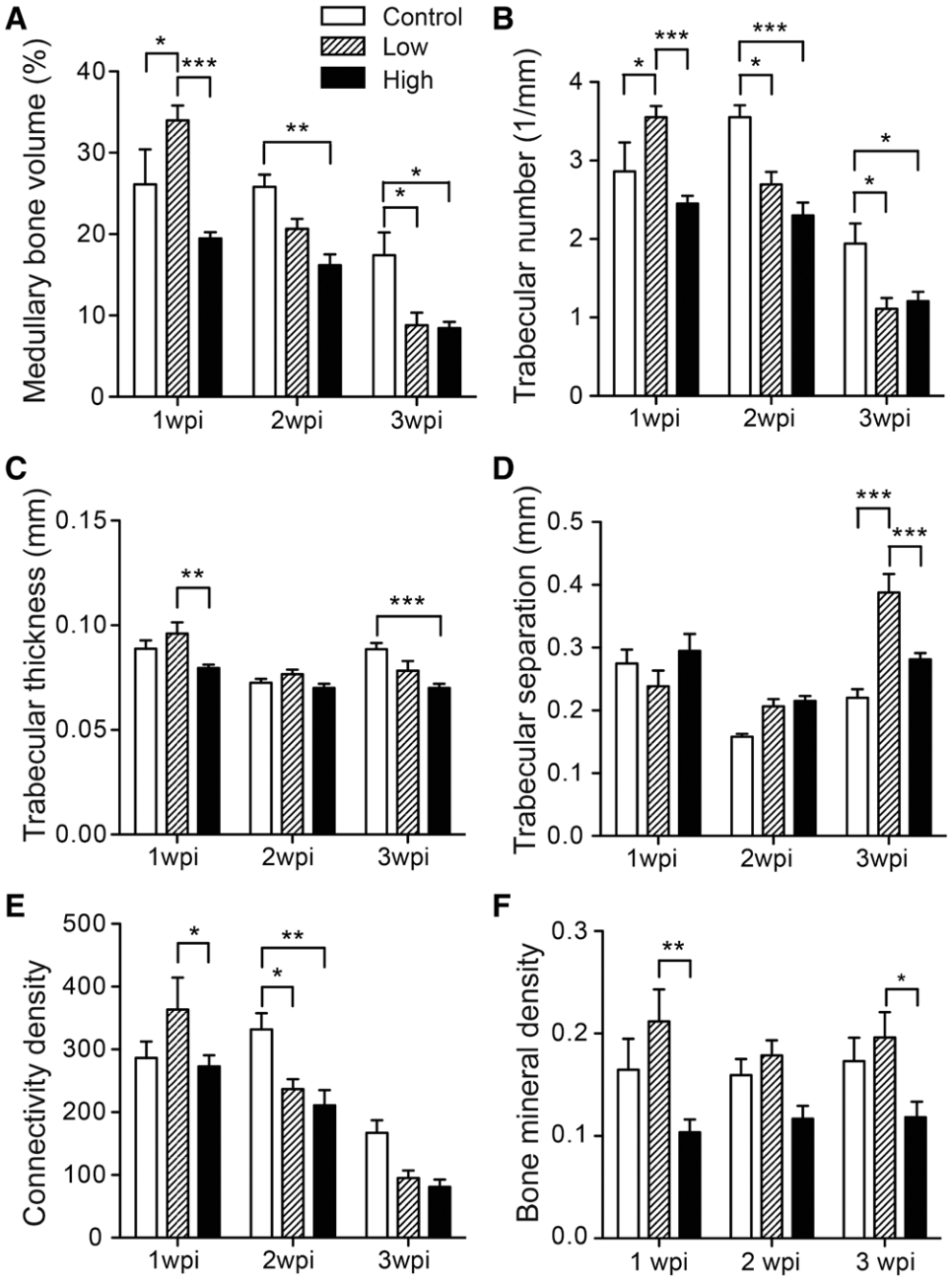

Fig. 3 Morphometric and densitometric analysis of μCT. The generation of trabecular bone increased early in the bone healing process and decreased at the later stage as measured by medullary BV/TV (A) and trabecular number (B). Trabecular thickness (C) and trabecular separation (D) represent the morphology of the trabecular bone. The overall complexity of trabecular bone decreased as the remodeling progressed during the later stage of bone healing as measured by connectivity density (E). Bone mineral density (F) usually correlates with the strength of the bone. (*$p < 0.05$, **$p < 0.01$, ***$p < 0.001$, n = 6). μCT = micro-computed tomographic; BV/TV = trabecular bone/tissue volume; wpi = weeks post-injury.

different between groups. The results of bone volume fraction in the medullary cavity, Tb. N, Tb. Th, and Conn.D peaked within the first 7 days for both the HPSE1 treatment groups but not for the control group. The bone volume fraction in the medullary cavity and Tb. N, both of which represent the generation of trabecular bones, remained at its peak value at 1 and 2 wpi in the control group, while showing a marked decreased trend after 1 wpi in both the HPSE1-treated groups (**Fig. 3A, B**). A similar trend could also be observed in the Conn.D (**Fig. 3E**), which represents the complexity of the trabecular bones. Moreover, the highest values of Tb. N and Conn.D are at comparable levels in the low-dose HPSE1-treated group and the control group, although at different time points. Collectively, these data indicated that the progress of bone healing was accelerated by the presence of HPSE1. Interestingly, these values showed the same pattern in both the HPSE1-treated groups throughout the study period but were significantly lower in the high-dose group than in the low-dose group at 1 wpi, implying that the peak value in the high-dose group was attained within 7 days after the injury.

Although bone healing progress is accelerated by the presence of HPSE1, the overall healing results in the HPSE1 high-dose group were not superior to the low-dose group and fared

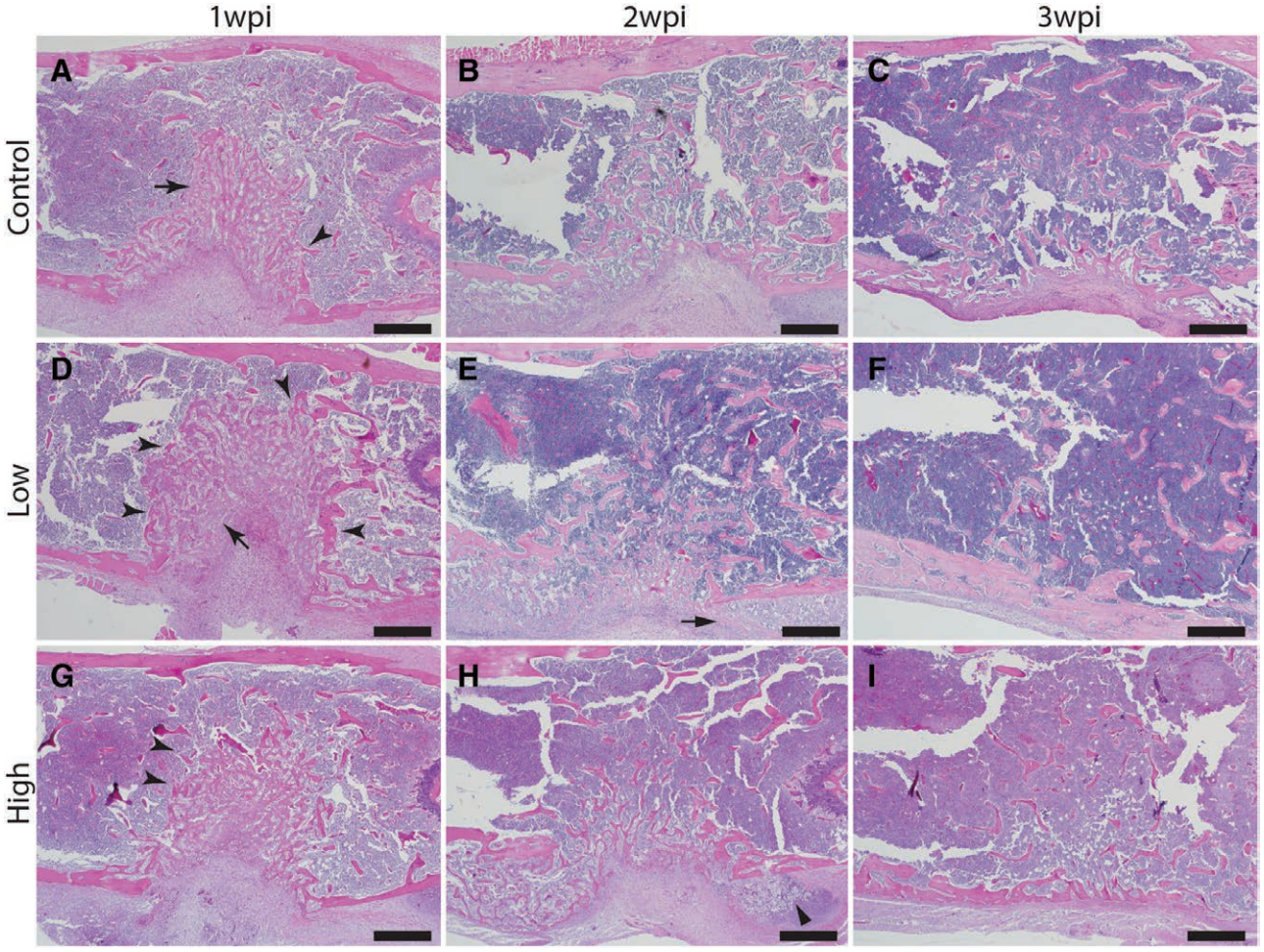

Fig. 4 Representative micrographs of bone defect in the control group (Control) and heparanase-treated groups (High and Low) at 1, 2, and 3 wpi. Typical histological changes include the generation of fibrous woven bones (concave arrows) and trabecular bones (concave arrowheads) in the medullary cavity at the early healing stage (1 wpi; A, D, G), ossification and remodeling at the mid-stage (2 wpi; B, E, H), and the restoration of cortical bones at the late stage (3 wpi; C, F, I). The markedly enriched trabecular bone (concave arrowheads) in the low-dose HPSE1 group at 1 wpi (D) and hypertrophic chondrocytes (arrowhead) in the high-dose HPSE1 group at 2 wpi could be easily observed (H). At 3 wpi, the cortical bone in the low-dose HPSE1-treated group (F) appeared thicker than in the other groups (C, I). Scale bar = 500 μm. HPSE = heparanase; wpi = weeks post-injury.

Table

Histological features of bone healing progress in different treatment groups

	Control			HPSE1-Low			HPSE1-High		
	7	14	21	7	14	21	7	14	21
Medullary bone fraction	++	++	+	+++	++	+/–	++	+	+/–
Cortical bridging	–	+/–	+	–	+	++	–	+	++
Cartilage tissue	0/6	3/6	2/6	0/6	5/6	2/6	0/6	6/6	2/6

HPSE = heparanase.

even worse as measured by BMD on μCT (**Fig. 3F**) and cortical bone volume fraction on histomorphometry (**Fig. 5**), implying a biphasic effect of HPSE1. In addition to osteogenic effects, HPSE has also been found to stimulate receptor activation of nuclear factor kappa-B ligand (RANKL) expression, which triggers osteoclastogenesis and promotes osteolysis.[25] Furthermore, cross-talk between osteoclasts and osteoblasts has been proposed.[26,27] In principle, osteoblasts can either promote the activation of osteoclasts via monocyte/macrophage colony-stimulating factor (M-CSF), RANKL, and WNT5A or inhibit osteoclasts via osteoprotegerin (OPG), Semaphorin (SEMA) 3A, and WNT16.[26,28–31] On the other hand, osteoclasts can recruit osteoblasts at sites of bone remodeling through factors such as BMP-6, collagen triple helix repeat containing 1 (CTHRC1), Ephrin-B2, sphingosine-1-phosphate (S1P), WNT10B, SEMA4D, and cardiotrophin-1 (CT-1).[32–36] It is speculated that low-dose HPSE1 activates osteoclasts to the extent that an optimum balance is maintained between osteoclasts and osteoblasts and therefore enhance the dynamics of bone remodeling during the healing process without compromising the resulting BMD and cortical bone volume fraction at the end point. However, although a high dose of HPSE1 activates osteoclasts and in turn facilitates the progression of

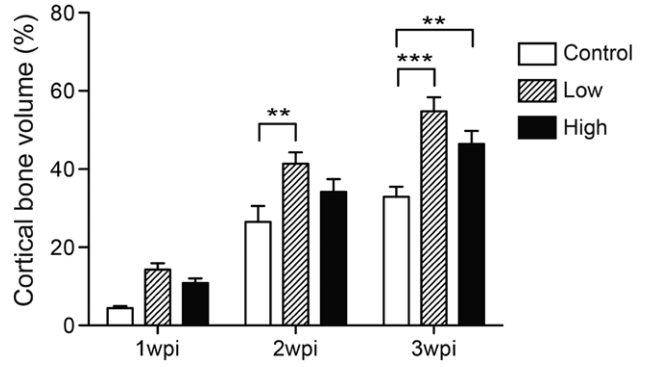

Fig. 5 Morphometric analysis of cortical bone volume fraction indicated that HPSE1 treatment augments the thickness of cortical bone at 3 wpi. (**$p < 0.01$, ***$p < 0.001$, n = 6). HPSE = heparanase; wpi = weeks post-injury.

bone remodeling during bone healing, the resulting BMD and cortical bone volume fraction at the end point are also significantly lower. Although this is the first attempt at the application of HPSE1 for bone healing, the high-dose group (12.5 μg/d) in our study was at a relatively higher dosage compared with other studies, despite the route of administration, target tissues, and frequency of HPSE administration varying considerably.[13,37,38] HPSE might tip the balance toward osteoclastogenesis when the dosage is too high. For further delineating the biphasic effect of HPSE1, especially determining the optimal dose, the evaluation of more groups at different dosages is required. However, the purpose of this study was to confirm the effect of HPSE1 on bone healing. Further studies are warranted to understand the detailed biphasic effect and optimal dose of HPSE1 in bone healing. Interestingly, patients with type 2 diabetes have significantly higher blood HPSE1 levels than healthy individuals,[39] while they also have a higher cortical porosity with risk for fragility fractures.[40] Therefore, the administrative routes, dose, and period of application of HPSE1 for bone healing should be carefully studied and optimized. This is also why the topical infusion of HPSE1 was chosen for the experiments in the present study, instead of systemic routes. The topical application of HPSE1 allows observation of the effects without systemic complication, if any.

The bone regeneration in the model used in the present study was mainly intramembranous ossification with partial endochondral ossification. In previous studies with this model, endochondral ossification was observed in some cases with temporal succession of cartilage, hypertrophic and mineralized cartilage.[17] This not only was observed in our study, but also both the HPSE1-treated groups demonstrated a higher rate of cartilage formation than the control group at 2 wpi (Table). Interestingly, a previous study showed that HPSE1 was highly expressed during chondrocyte differentiation and enzymatic inhibition of HPSE1 reduced the chondrogenesis.[41] Although there is no evidence indicating whether the ossification process affects the outcomes of bone healing, it is plausible that HPSE1 promotes endochondral ossification during bone healing.

In the present study, we showed that the topical infusion of exogenous HPSE1 could accelerate the progress of bone healing. Our findings suggest that an appropriate amount of HPSE1 may also strengthen the cortical bone and, in turn, augment the healing outcome. Therefore, HPSE1 is a potential therapeutic target for bone injuries and fractures. In future, it is critical to study and determine the optimal dosage, route, and application period required to prevent the occurrence of potential adverse effects in the event of overdose.

ACKNOWLEDGMENTS

The authors would like to thank Dr. Shau-Ping Lin for the assistance on the development of this project, Ms. Kai-Han Lin and Ms. Ke-Hsuan Wei for heparanase preparation, and Ms. Yen-Hua Lee and Dr. Chun-Chun Cheng for technical support on animal handling. We also thank the Taiwan Mouse Clinic (102-2325-B-001-042) which is funded by the National Research Program for Biopharmaceuticals (NRPB) at the Ministry of Science and Technology (MOST) of Taiwan for technical support in the acquisition and analysis of the micro-computed tomographic (μCT) data. This work was funded by Ministry of Science and Technology, Taiwan to I-Hsuan Liu (100-2313-B-002-052-MY2, 105-2628-B-002-005-MY4), Winston Teng-Kuei Cheng (102-2313-B-029-002), and Ya-Pei Chang (106-2313-B-002-041). The funding agency has no role in the experimental design, data acquirement, analysis, and interpretation of this work.

REFERENCES

1. Marsell R, Einhorn TA. The biology of fracture healing. *Injury* 2011;**42**:551–5.
2. Fazzalari NL. Bone fracture and bone fracture repair. *Osteoporos Int* 2011;**22**:2003–6.
3. Bishop JR, Schuksz M, Esko JD. Heparan sulphate proteoglycans fine-tune mammalian physiology. *Nature* 2007;**446**:1030–7.
4. Globus RK, Patterson-Buckendahl P, Gospodarowicz D. Regulation of bovine bone cell proliferation by fibroblast growth factor and transforming growth factor beta. *Endocrinology* 1988;**123**:98–105.
5. Street J, Bao M, deGuzman L, Bunting S, Peale FV Jr, Ferrara N, et al. Vascular endothelial growth factor stimulates bone repair by promoting angiogenesis and bone turnover. *Proc Natl Acad Sci U S A* 2002;**99**:9656–61.
6. Yasko AW, Lane JM, Fellinger EJ, Rosen V, Wozney JM, Wang EA. The healing of segmental bone defects, induced by recombinant human bone morphogenetic protein (rhBMP-2). A radiographic, histological, and biomechanical study in rats. *J Bone Joint Surg Am* 1992;**74**:659–70.
7. Bramono DS, Murali S, Rai B, Ling L, Poh WT, Lim ZX, et al. Bone marrow-derived heparan sulfate potentiates the osteogenic activity of bone morphogenetic protein-2 (BMP-2). *Bone* 2012;**50**:954–64.
8. Gdalevitch M, Kasaai B, Alam N, Dohin B, Lauzier D, Hamdy RC. The effect of heparan sulfate application on bone formation during distraction osteogenesis. *PLoS One* 2013;**8**:e56790.
9. Jackson RA, McDonald MM, Nurcombe V, Little DG, Cool SM. The use of heparan sulfate to augment fracture repair in a rat fracture model. *J Orthop Res* 2006;**24**:636–44.
10. Freeman C, Parish CR. Human platelet heparanase: purification, characterization and catalytic activity. *Biochem J* 1998;**330**(Pt 3):1341–50.
11. Vlodavsky I, Friedmann Y, Elkin M, Aingorn H, Atzmon R, Ishai-Michaeli R, et al. Mammalian heparanase: gene cloning, expression and function in tumor progression and metastasis. *Nat Med* 1999;**5**:793–802.
12. D'Souza S, Yang W, Marchetti D, Muir C, Farach-Carson MC, Carson DD. HIP/RPL29 antagonizes VEGF and FGF2 stimulated angiogenesis by interfering with HS-dependent responses. *J Cell Biochem* 2008;**105**:1183–93.
13. Elkin M, Ilan N, Ishai-Michaeli R, Friedmann Y, Papo O, Pecker I, et al. Heparanase as mediator of angiogenesis: mode of action. *FASEB J* 2001;**15**:1661–3.
14. Kram V, Zcharia E, Yacoby-Zeevi O, Metzger S, Chajek-Shaul T, Gabet Y, et al. Heparanase is expressed in osteoblastic cells and stimulates bone formation and bone mass. *J Cell Physiol* 2006;**207**:784–92.
15. Park D, Spencer JA, Koh BI, Kobayashi T, Fujisaki J, Clemens TL, et al. Endogenous bone marrow MSCs are dynamic, fate-restricted participants in bone maintenance and regeneration. *Cell Stem Cell* 2012;**10**:259–72.
16. Cheng CC, Lee YH, Lin SP, Huangfu WC, Liu IH. Cell-autonomous heparanase modulates self-renewal and migration in bone marrow-derived mesenchymal stem cells. *J Biomed Sci* 2014;**21**:21.
17. Uusitalo H, Rantakokko J, Ahonen M, Jämsä T, Tuukkanen J, KäHäri V, et al. A metaphyseal defect model of the femur for studies of murine bone healing. *Bone* 2001;**28**:423–9.
18. Bouxsein ML, Boyd SK, Christiansen BA, Guldberg RE, Jepsen KJ, Müller R. Guidelines for assessment of bone microstructure in rodents using micro-computed tomography. *J Bone Miner Res* 2010;**25**:1468–86.

19. Schneider CA, Rasband WS, Eliceiri KW. NIH image to imagej: 25 years of image analysis. *Nat Methods* 2012;**9**:671–5.
20. Giannoudis PV, Einhorn TA, Marsh D. Fracture healing: the diamond concept. *Injury* 2007;**38**(Suppl 4):S3–6.
21. Keramaris NC, Calori GM, Nikolaou VS, Schemitsch EH, Giannoudis PV. Fracture vascularity and bone healing: a systematic review of the role of VEGF. *Injury* 2008;**39**(Suppl 2):S45–57.
22. Goldberg R, Meirovitz A, Hirshoren N, Bulvik R, Binder A, Rubinstein AM, et al. Versatile role of heparanase in inflammation. *Matrix Biol* 2013;**32**:234–40.
23. Parish CR, Freeman C, Hulett MD. Heparanase: a key enzyme involved in cell invasion. *Biochim Biophys Acta* 2001;**1471**:M99–108.
24. Patel VN, Knox SM, Likar KM, Lathrop CA, Hossain R, Eftekhari S, et al. Heparanase cleavage of perlecan heparan sulfate modulates FGF10 activity during ex vivo submandibular gland branching morphogenesis. *Development* 2007;**134**:4177–86.
25. Yang Y, Ren Y, Ramani VC, Nan L, Suva LJ, Sanderson RD. Heparanase enhances local and systemic osteolysis in multiple myeloma by upregulating the expression and secretion of RANKL. *Cancer Res* 2010;**70**:8329–38.
26. Han Y, You X, Xing W, Zhang Z, Zou W. Paracrine and endocrine actions of bone-the functions of secretory proteins from osteoblasts, osteocytes, and osteoclasts. *Bone Res* 2018;**6**:16.
27. Sims NA, Walsh NC. Intercellular cross-talk among bone cells: new factors and pathways. *Curr Osteoporos Rep* 2012;**10**:109–17.
28. Fuller K, Owens JM, Jagger CJ, Wilson A, Moss R, Chambers TJ. Macrophage colony-stimulating factor stimulates survival and chemotactic behavior in isolated osteoclasts. *J Exp Med* 1993;**178**:1733–44.
29. Hayashi M, Nakashima T, Taniguchi M, Kodama T, Kumanogoh A, Takayanagi H. Osteoprotection by semaphorin 3A. *Nature* 2012;**485**:69–74.
30. Kong YY, Yoshida H, Sarosi I, Tan HL, Timms E, Capparelli C, et al. OPGL is a key regulator of osteoclastogenesis, lymphocyte development and lymph-node organogenesis. *Nature* 1999;**397**:315–23.
31. Simonet WS, Lacey DL, Dunstan CR, Kelley M, Chang MS, Lüthy R, et al. Osteoprotegerin: a novel secreted protein involved in the regulation of bone density. *Cell* 1997;**89**:309–19.
32. Ota K, Quint P, Ruan M, Pederson L, Westendorf JJ, Khosla S, et al. TGF-β induces wnt10b in osteoclasts from female mice to enhance coupling to osteoblasts. *Endocrinology* 2013;**154**:3745–52.
33. Pederson L, Ruan M, Westendorf JJ, Khosla S, Oursler MJ. Regulation of bone formation by osteoclasts involves wnt/BMP signaling and the chemokine sphingosine-1-phosphate. *Proc Natl Acad Sci U S A* 2008;**105**:20764–9.
34. Ryu J, Kim HJ, Chang EJ, Huang H, Banno Y, Kim HH. Sphingosine 1-phosphate as a regulator of osteoclast differentiation and osteoclast-osteoblast coupling. *EMBO J* 2006;**25**:5840–51.
35. Takeshita S, Fumoto T, Matsuoka K, Park KA, Aburatani H, Kato S, et al. Osteoclast-secreted CTHRC1 in the coupling of bone resorption to formation. *J Clin Invest* 2013;**123**:3914–24.
36. Zhao C, Irie N, Takada Y, Shimoda K, Miyamoto T, Nishiwaki T, et al. Bidirectional ephrinb2-EphB4 signaling controls bone homeostasis. *Cell Metab* 2006;**4**:111–21.
37. Bitan M, Weiss L, Zeira M, Reich S, Pappo O, Vlodavsky I, et al. Heparanase prevents the development of type 1 diabetes in non-obese diabetic mice by regulating T-cell activation and cytokines production. *Diabetes Metab Res Rev* 2008;**24**:413–21.
38. Zcharia E, Zilka R, Yaar A, Yacoby-Zeevi O, Zetser A, Metzger S, et al. Heparanase accelerates wound angiogenesis and wound healing in mouse and rat models. *FASEB J* 2005;**19**:211–21.
39. Shafat I, Ilan N, Zoabi S, Vlodavsky I, Nakhoul F. Heparanase levels are elevated in the urine and plasma of type 2 diabetes patients and associate with blood glucose levels. *PLoS One* 2011;**6**:e17312.
40. Patsch JM, Burghardt AJ, Yap SP, Baum T, Schwartz AV, Joseph GB, et al. Increased cortical porosity in type 2 diabetic postmenopausal women with fragility fractures. *J Bone Miner Res* 2013;**28**:313–24.
41. Brown AJ, Alicknavitch M, D'Souza SS, Daikoku T, Kirn-Safran CB, Marchetti D, et al. Heparanase expression and activity influences chondrogenic and osteogenic processes during endochondral bone formation. *Bone* 2008;**43**:689–99.